Growth of Rubrene thin film, spherulites and nanowires on SiO2

ARTICLE *in* PHYSICA STATUS SOLIDI (A) APPLICATIONS AND MATERIALS · JUNE 2007

Impact Factor: 1.62 · DOI: 10.1002/pssa.200675340

Original Paper

phys. stat. sol. (a) **204**, No. 6, 1851–1855 (2007) / **DOI** 10.1002/pssa.200675340

Growth of Rubrene thin film, spherulites and nanowires on SiO_2

Y. Luo[1], **M. Brun**[2], **P. Rannou**[1], and **B. Grevin**[*, 1]

[1] CEA-Grenoble, DRFMC, UMR5819-SPrAM (CEA-CNRS-Univ. J. Fourier-Grenoble I), LEMOH, 17 Rue des Martyrs, 38 054 Grenoble Cedex 9, France
[2] CEA-LETI, MINATEC, 17 Rue des Martyrs, 38 054 Grenoble Cedex 9, France

Received 16 October 2006, revised 29 January 2007, accepted 5 February 2007
Published online 23 May 2007

PACS 68.37.Hk, 68.37.Ps, 72.80.Le, 81.07.Nb, 81.10.Aj, 81.15.Ef

The growth of rubrene thin films thermally evaporated under ultra-high vacuum (UHV) on SiO_2 has been investigated by combining atomic force microscopy (AFM), scanning electron microscopy (SEM), and polarized optical microscopy (POM) techniques. A mode of thin film growth in which an amorphous continuous holy film first covers the substrate, and acts afterwards as a template for the nucleation of polycrystalline rubrene spherulites, has been identified. Additionally, rubrene one-dimensional structures have been observed with a catalyst-free growth process.

1 Introduction

Organic semiconductors have been widely studied for the realization of electronic devices such as organic light-emitting diodes (OLEDs) [1], organic field-effect transistors (OFETs) [2], and thin film organic photovoltaic cells [3]. Amongst these materials, rubrene ($C_{42}H_{28}$: 5,6,11,12-tetraphenylnaphthacene) has recently emerged as a very promising candidate for high performances single-crystal OFETs (SCOFETs) [4–5]. Rubrene is a pi-conjugated molecule consisting of a tetracene backbone with four phenyl side groups as depicted in Fig. 1a. In its crystalline state, its chemical structure and structural packing make it less sensitive than other organic semiconductors to contamination effects by oxygen or chemical impurities. In addition to be considered as a very important dopant for yellow and white OLEDs [6, 7], high carrier mobility values (~15 $cm^2\ V^{-1}\ s^{-1}$ at room temperature) have been reported for rubrene SCOFETs [4, 5]. However, OFETs based on thin films are highly desirable, for the development of large area, low-cost, and flexible electronic devices [3, 8]. In that sense, pentacene, which can display field-effect mobilities values exceeding 1 $cm^2\ V^{-1}\ s^{-1}$ in thin films-based OFETs [9, 10], seemed to be more suited than rubrene for the realization of operational thin film-based OFETs. For rubrene, so far, no high performances thin film OFETs have been achieved by conventional deposition techniques and the development of new strategies is needed [11]. Compared with single crystal growth, the fabrication of highly ordered crystalline rubrene thin films by evaporation on substrates, such as SiO_2, is indeed an intrinsically difficult task. Its complex molecular conformation [12] results in the formation of a disordered seed layer on the substrate, which prevents the later growth of an ordered thin film.

In the present study we focus on the growth of rubrene thin films on SiO_2 and demonstrate the novel rubrene spherulitic structure and nanowires when the substrate temperature is higher than 80 °C during the growth. We investigate a mode of thin film growth (depicted in Fig. 1b) in which an amorphous continuous holy film first covers the substrate, and acts afterwards as a template for the nucleation of polycrystalline spherulites [13, 14]. The length of the micro-crystalline domains inside rubrene spheruli-

[*] Corresponding author: e-mail: benjamin.grevin@cea.fr, Phone: +33 (0)4 38 78 46 15, Fax: +33 (0)4 38 78 51 13

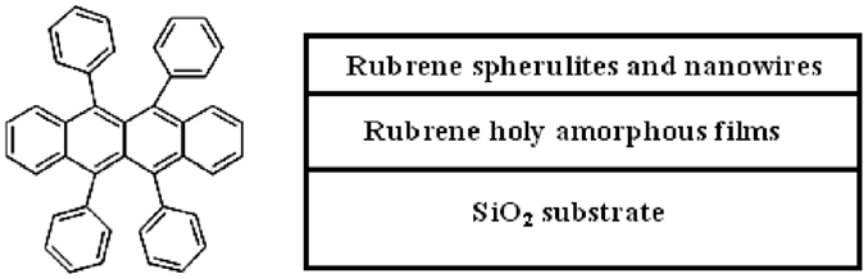

Fig. 1 a) Chemical structure of rubrene. b) Schematic cross section of rubrene thin film growth.

tes is up to 10 μm, which may provide a new route for the fabrication of top-gated OFET devices based on single rubrene domain. Interestingly, rubrene one-dimensional structures have been observed on the top layers, which could pave the way towards the investigation of electronic transport properties of rubrene's nanowire-based OFETs.

2 Experimental

Rubrene was purchased from Aldrich (purity >99%) and was used as received. Thermally grown silicon dioxide was used as the substrate. The wafer was thoroughly cleaned by ultra-sonication in acetone and ethanol, respectively. Thin films were thermally evaporated in an UHV system with a base pressure of ca. 10^{-9} mbar. Rubrene was sublimed from a Knudsen cell mounted toward the sample holder. The substrate temperature was precisely controlled in the 25–100 °C temperature range by using an *in situ* CrAl thermocouple. The structure and surface morphology of the films were characterized by AFM (Nanotec Electronica, Spain) operating in tapping mode under ambient conditions, SEM (MEB ZEISS Ultra 55, Germany), and POM (Olympus BX60, Japan).

3 Results and discussion

Figure 2 presents AFM images of rubrene thin films grown at a substrate temperature of 85 °C with different deposited thickness. In contrast to single-crystals growth by vapour phase method, 3-dimentional islands were formed on SiO_2 substrates. When rubrene molecules land on the surface, the sum of

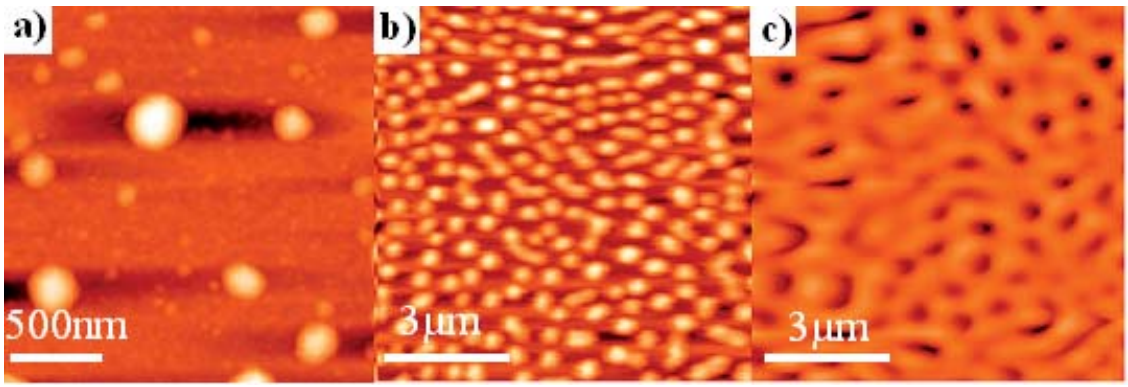

Fig. 2 (online colour at: www.pss-a.com) AFM images of rubrene three-dimensional islands grown on SiO_2 at a substrate temperature of 85 °C with different deposited thickness. a) Isolated islands at initial growth stage. b) Coalesced islands at higher coverage. c) Continuous holy film.

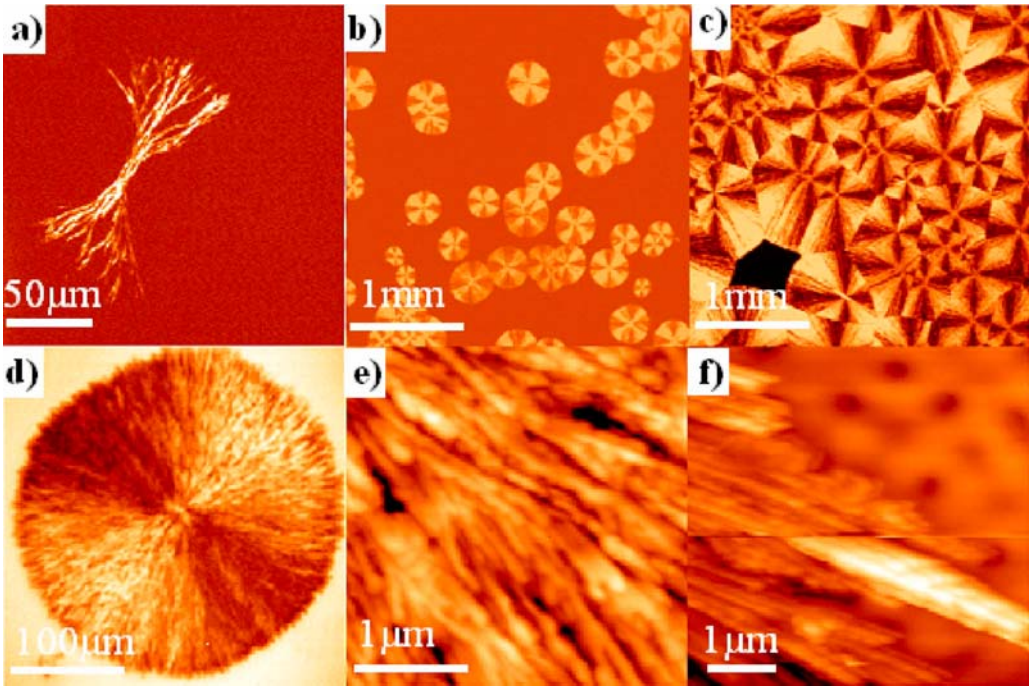

Fig. 3 (online colour at: www.pss-a.com) Rubrene spherulites growth on a "template" layer. a–d) POM images at different stages of the spherulites growth process. e) AFM image of rubrene threadlike crystal fibers inside the spherulites. f) AFM image of the edge of spherulites, indicating the interface between spherulites and the "template" layer. The substrate temperature is in the 82–90 °C temperature range, while the pressure is of ca. 10^{7} mbar.

the rubrene free energy γ_{ru} and effective interfacial energy γ^* is larger than SiO_2 substrate free energy γ_{sub}: $\gamma_{ru} + \gamma^* > \gamma_{sub}$. Therefore, an island-growth mode (Volmer–Weber mode) is favoured, rather than a layer-by-layer one (Frank van der Merve mode). Moreover, from the AFM images and the corresponding profiles (not shown), these islands are associated to an amorphous phase of rubrene, which is consistent with the occurrence of random conformations for the first molecules adsorbed at the substrate interface [12].

Following their nucleation, these rubrene islands continuously grow in the three dimensions from the height of ca. 12~16 nm (Fig. 2a) up to that of ca. 60~80 nm (Fig. 2b), while their width reach a limit of ca. 150~200 nm. Increasing the quantity of deposited material above a critical coverage density triggers the formation of a network of coalesced islands (Fig. 2b) which latter on end up with a continuous holy rubrene thin film (Fig. 2c). The depth of the holes is equal to the height of the islands, i.e. 60~80 nm while the shape and the width are not uniform. Interestingly, we identified a subsequent growth step, i.e. the formation of polycrystalline rubrene spherulites grown on the top of the previously formed continuous holy thin film which acts as a "template" layer [13, 14]. This subsequent growth step is only observed when the substrate temperature is higher than 80 °C.

The formation of spherulites is ubiquitous in solids formed by quenching a liquid phase into a crystalline solid state under high non-equilibrium conditions [15]. Many materials, such as metal alloys, polymers, and minerals, can form spherulites [16–18]. Several phenomenological models and physical conditions have been suggested [19, 20]. However, the observations and associated models are generally based on growth processes in the frame of liquid–solid methods. In this study, the substrate temperature was fixed at 85 °C, far from the melting point of rubrene (~334 °C). Therefore, the spherulitic growth observed in our case seems somehow unconventional, especially because it involves an holy "template"

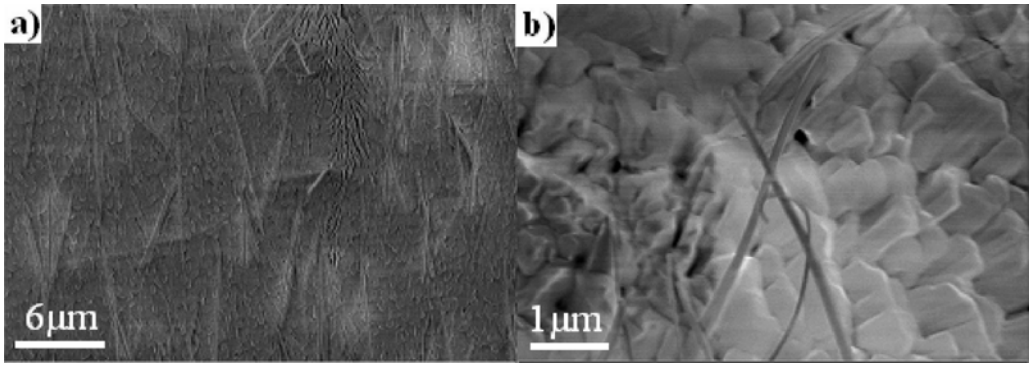

Fig. 4 a), b) SEM images of rubrene nanowires grown on rubrene thin films. The deposition condition is the same as the samples shown in Fig. 3.

layer of the same material. In that sense, it totally differs from the growth of free-standing single crystals (in the layer-by-layer mode) and from the one of totally amorphous films (in the island mode).

Figure 3 displays different snapshots (POM and AFM images) of the complex growth process of rubrene polycrystalline spherulites seeded on the top of an amorphous and holy rubrene thin film which seems to be consistent with one reported spherulites growth mode [20]. The initial growth starts with the appearance of threadlike fibers, which subsequently form crystalline "sheaves", as shown in Fig. 3a. This two-end branched growth is anisotropic and "sheaves" splays out continuously during the growth until a rough spherical shape emerges (Fig. 3b–d). The nucleation of rubrene spherulites is homogenous, and both their density and coverage can be controlled by the deposition parameters (respectively the rate and thickness). By increasing the amount of deposited material, a coalescence of spherulites occurs and span over the whole substrate as shown in Fig. 3c.

As discussed above, rubrene spherulites consist of branches of crystal "sheaves". Figure 3e, f show the AFM images of these structures, which consist in ordered threadlike domain. The length of these 100–300 nm wide single domains is up to 10 μm, which is sufficient to be covered by thermally evaporated source and drain electrodes using shadow mask. These results suggest a way to realize OFETs based on polycrystalline rubrene spherulite active layer with both top contacts and top-gate configurations. Recently, some top-gated OFETs have been reported, in which polymer gate dielectrics were used [21, 22], and such a configuration seems to be well-adapted for studying electronic properties of rubrene spherulites-based OFETs.

Finally, besides these spherulitic structures, SEM images (Fig. 4) suggest the existence of unprevioulsy observed rubrene nanowires with length up to 10 micrometers and width of ca. 50–100 nm. For many materials, the use of a catalyst in the vapour–liquid–solid (VLS) or vapour–solid–solid (VSS) [23] is required for the synthesis of nanowires. Here, the growth process would have to be a self-catalytic one, starting either from the spherulites or even possibly from the holy "template" rubrene amorphous layer [13, 14]. From SEM investigations, the wires grow randomly and some of them stand vertically. As shown in Fig. 4b), these quasi-one dimensional structures can be bent and their apparent thickness is homogeneous. Their lengths can reach up to 10 μm with lateral dimensions in the 50–150 nm ranges. These separated nanowires are not the same as fibers inside the spherulitic structures, which have larger width and different top morphologies. Future work will focus on the study of this particular growth mode and the structural perfection of these quasi-one dimensional self-assembled rubrene-based semiconducting structures.

4 Conclusions

In conclusion, rubrene thin film growth on SiO_2 by evaporation under UHV has been investigated by combining AFM, SEM, and POM. We have shown that the initial growth of an amorphous holy layer

grown at 85 °C (under ultra-high vacuum) can act as a template for the nucleation and growth of polycrystalline rubrene spherulites consisting of ordered crystalline-threadlike domains. SEM images suggest also the formation of previously unreported rubrene nanowires which could be potentially used for the fabrication of rubrene nanowires-based OFETs.

Acknowledgements This work has been performed in the framework of the ACI grant "TrENTO" sponsored by the French Ministry of Research in joint collaboration between UMR5819-SPrAM, CEA-Grenoble DRFMC/SPSMS, and UMR8520-IEMN. This work was also in part supported by the Micro and Nanotechnology Program from the French Ministry of Research under the grant "RTB: Post CMOS moléculaire 200 mm" (head of this program at CEA-grenoble: Dr. Robert Baptist). The authors are grateful to Dr. Thierry Livache for the the use of the polarized optical microscope used in this work and thanks Prof. Peter Beton and Dr. Martin Brinkmann for useful discussions.

References

[1] U. Mitschke and P. Baüerle, J. Mater. Chem. **10**, 1471 (2000).
[2] H. Sirringhaus, Adv. Mater. **17**, 2411 (2005).
[3] S. R. Forrest, Nature **428**, 911 (2004).
[4] A. L. Briseno, R. J. Tseng, M.-M. Ling, E. H. L. Falcao, Y. Yang, F. Wudl, and Z. Bao, Adv. Mater. **18**, 2320 (2006).
[5] M. E. Gershenson, V. Podzorov, and A. F. Morpurgo, Rev. Mod. Phys. **78**, 973 (2006).
[6] Y. Hamada, H. Kanno, T. Tsujioka, H. Takahashi, and T. Usuki, Appl. Phys. Lett. **75**, 1682 (1999).
[7] C. H. Chuen and Y. T. Tao, Appl. Phys. Lett. **81**, 4499 (2002).
[8] C. D. Dimitrakopoulos and P. R. L. Malenfant, Adv. Mater. **14**, 99 (2002).
[9] Y.-Y. Lin, D. J. Gundlach, T. N. Jackson, and S. F. Nelson, IEEE Trans. Electron. Devices **44**, 1325 (1997).
[10] G. Wang, Y. Luo, and P. H. Beton, Appl. Phys. Lett. **83**, 3108 (2003).
[11] N. Stingelin-Stutzmann, E. Smits, H. Wondergem, C. Tanase, P. Blom, P. Smith, and D. de Leeuw, Nature Mater. **4**, 601 (2005).
[12] D. Kafer, L. Ruppel, G. Witte, and Ch. Woll, Phys. Rev. Lett. **95**, 166602 (2005).
[13] A. J. Page and R. P. Sear, Phys. Rev. Lett. **97**, 065701 (2006).
[14] D. Frenkel, Nature **443**, 641 (2006).
[15] J. H. Magill, J. Mater. Sci. **36**, 3143 (2001).
[16] G. Ryschenkow and G. Faivre, J. Non-Cryst. Solids **87**, 221 (1988).
[17] H. W. Morse, C. H. Warren, and J. D. H. Donnay, Am. J. Sci. **23**, 421 (1932).
[18] D. C. Bassett, Principles of polymer morphology (Cambridge University Press, New York, 1981).
[19] J. L. Hutter and J. Bechhoefer, Phys. Rev. E **59**, 4342 (1999).
[20] L. Granasy, T. Pusztai, G. Tegze, J. A. Warren, and J. F. Douglas, Phys. Rev. E **72**, 11605 (2005).
[21] C. R. Newman, R. J. Chesterfield, M. J. Panzer, and C. D. Frisbie, J. Appl. Phys. **98**, 84506 (2005).
[22] M. Ling, Z. Bao, and D. Li, Appl. Phys. Lett. **88**, 33502 (2006).
[23] Y. Xia, P. Yang, Y. Sun, Y. Wu, B. Mayers, B. Gates, Y. Yin, F. Kim, and H. Yan, Adv. Mater. **15**, 353 (2003).

